Chemical Engineering Journal 166 (2011) 168–175

Contents lists available at ScienceDirect

Chemical Engineering Journal

journal homepage: www.elsevier.com/locate/cej

Influence of the polyethyleneimine grafting on the adsorption capacity of chitosan beads for Reactive Black 5 from aqueous solutions

Sudipta Chatterjee, Tania Chatterjee, Seung H. Woo*

Department of Chemical Engineering, Hanbat National University, San 16-1, Deokmyeong-Dong, Yuseong-Gu, Daejeon 305-719, Republic of Korea

ARTICLE INFO

Article history:
Received 25 July 2010
Received in revised form 16 October 2010
Accepted 18 October 2010

Keywords:
Chitosan bead
Polyethyleneimine
Reactive Black 5
Grafting
Adsorption
Sodium dodecyl sulphate

ABSTRACT

The adsorption capacity of chitosan hydrogel beads generated by alkali (CB) and sodium dodecyl sulphate (CSB) gelation was investigated after polyethyleneimine (PEI) grafting for adsorption of Reactive Black 5 (RB5) from aqueous solutions. The adsorption capacities of PEI-grafted CB (PEI-CB) and CSB (PEI-CSB) were varied with the amount of PEI used during grafting. The maximum adsorption capacity values of PEI-CB (709.27 mg/g) and PEI-CSB (413.23 mg/g) obtained from the Langmuir isotherm model were higher than those of CB (201.90 mg/g) and CSB (168.07 mg/g), indicating that the adsorption performance of CB and CSB could be highly enhanced by PEI grafting. All of the adsorption systems showed better fits to the Langmuir isotherm model than the Freundlich isotherm model, except PEI-CSB. The kinetic data of the adsorption systems showed better fits to a pseudo-first-order rate model than a pseudo-second-order model.

1. Introduction

The large quantities of colored effluent discharged from textile, paper, plastic, leather, cosmetics, food and mineral processing industries has become a significant environmental problem [1]. These industries utilize more than 1000 dyes and pigments for coloring their products, and it is estimated that around 15% of the dyes is lost during dyeing and finishing processes [2]. Dye-containing water is one of the most important indicators of water pollution, and discharge of dyeing effluent into a watercourse is also aesthetically undesirable [3]. Among the many varieties of synthetic dyes, reactive dyes are the most toxic and mutagenic, and even carcinogenic, in nature [4,5]. Conventionally, physical, chemical and biological methods are adopted for the removal of dyes from colored effluents, but biological treatments are not found to be very successful due to the nonbiodegradable nature of most dyes [3]. Dye removal by adsorption is a simple physical method for dye removal from water, and various low cost adsorbents are found to be very effective because of their simplicity and high efficiency [6,7].

Nowadays, chitosan (CS)-based adsorbents have been intensely studied for the removal of dye molecules because of their low-cost, abundant availability, non-toxicity and potential for ion exchange [8]. CS is a naturally occurring linear biopolymer composed mostly of glucosamine and a small amount of N-acetyl glucosamine. It can be obtained on an industrial scale from chitin, because a large amount of crustacean's exoskeleton is available as a by-product of food processing industries. CS shows high adsorption capacity towards many classes of dyes because of multiple functional groups [9]. A recent review on environmental applications of CS for dye removal from aqueous solutions stated that CS-based adsorbents in the form of hydrogel beads exhibit the highest adsorption capacity for numerous dyes [8]. However, serious impediments to the practical applications of CS hydrogel beads are their low mechanical strength, solubility under acidic conditions and deformation after drying [8]. CS hydrogel beads formed by sodium dodecyl sulphate (SDS) gelation (CSB) exhibit better mechanical and acid stability than CS beads formed by alkali gelation [10], and CSB formation involves a simple process of dropwise addition of CS in acetic acid solution to SDS solution. This gelation method mainly involves multiple interactions such as electrostatic, ion-dipole and hydrophobic interactions between CS and SDS molecules [11–13].

The modification of CS-based adsorbents by grafting synthetic or natural polymers is a promising method for the preparation of novel CS-based materials and enables one to introduce special properties and expand the applications of CS-based materials in the environmental field [14]. CS derivative formed by grafting reactions was made mainly to enhance the density of reactive amine groups [14–16] or to improve its adsorption selectivity for adsorbates [17,18]. In this study, CS hydrogel beads formed by alkali gelation [19], and by SDS gelation [10], and their polyethyleneimine (PEI)-grafted derivatives were used for the adsorption of Reactive Black 5 (RB5), a model anionic dye, from aqueous solutions. RB5 is a black-colored diazo reactive vinylsulphonyl dye, and the

* Corresponding author. Tel.: +82 42 821 1537; fax: +82 42 821 1593.
E-mail address: shwoo@hanbat.ac.kr (S.H. Woo).

1385-8947/$ – see front matter © 2010 Elsevier B.V. All rights reserved.
doi:10.1016/j.cej.2010.10.047

adsorption of this dye has been widely studied using materials like activated carbon [20], agricultural waste products [21] and CS [22].

2. Experimental

2.1. Materials

CS (>85% deacetylation) obtained from crab shells, PEI, N,N,dimethyl acetamide (DMA), epichlorohydrin (ECH), SDS and RB5 were purchased from Sigma Chemical Co., USA. The molecular weight range reported for CS obtained from crab shells is 190–375 kDa and it comprises of medium high molecular weight CS [23]. PEI [$(-CH_2-CH_2-NH-)_n$] contains around 25% of primary amines, 50% and 25% of secondary and tertiary amines, respectively. All other chemicals of analytical grade were purchased from Sigma Chemical Co., USA.

2.2. Alkali and surfactant gelation

CS hydrogel bead formation by alkali gelation (CB) involved the dropwise addition of CS (1 wt%) in acetic acid solution (2 vol%) to alkali solution [19]. The development of CS hydrogel beads by SDS gelation (CSB) involved the dropwise (drop volume ~ 20 μl) addition of CS–acetic acid solution to 5 g/l of SDS solution [10]. To obtain the same SDS amount in CSB, a maximum of 20 beads were formed in 10 ml of SDS solution, and beads were collected from the same SDS solution after 3 h. Prepared beads were extensively washed with deionized water and preserved in an aqueous environment for future use.

2.3. Polyaminated CS beads formation by PEI grafting

For the synthesis of PEI-grafted CB (PEI-CB) and PEI-grafted CSB (PEI-CSB), 5 g of wet beads were added to 5 g of PEI dissolved in 100 ml of DMA solution in to exchange water with DMA and to favor the diffusion of PEI in the beads. The mixture was reacted while stirring (180 rpm) at 30 °C. After 24 h, the beads were rinsed with 30 ml of DMA and reacted with 0.5 ml of ECH (density 1.1812 g/ml) dissolved in 50 ml of DMA for 6 h at 60 °C. The PEI-grafted beads were then washed several times with deionized water to remove any unreacted material and stored in deionized water for further use. The polyamination of CB and CSB was also investigated using other PEI concentrations (1, 2.5, 10 and 15 g PEI in 100 ml of DMA solution).

2.4. Batch adsorption study

Several adsorption experiments using CB, PEI-CB, CSB and PEI-CSB were carried out under different experimental conditions for the adsorption of RB5 from aqueous solutions. All experiments were performed in 20-ml glass vials placed in a thermostat shaker operating at 150 rpm. In typical adsorption experiments, 0.2 g of wet beads were added to 10 ml of 500 mg/l of RB5 solution at 30 °C. All of the adsorption experiments were conducted in triplicate. The effect of PEI concentration variation (1, 2.5, 5, 10 and 15 g PEI/100 ml of DMA solution used for grafting 5 g of wet CB and CSB) on the adsorption capacity of the beads was studied. The effect of pH was studied after adjusting the initial pH of the dye solutions between 4 and 10 using dilute HCl and NaOH solutions. Kinetic adsorption experiments were carried out up to 1440 min to determine the equilibrium time for adsorption. Equilibrium adsorption experiments were carried out at different initial concentrations of RB5 (10–1000 mg/l) for CB and CSB and (10–3000 mg/l) for their PEI-grafted derivatives with an adsorption period of 24 h at 30 °C and pH 6. The PEI grafted CS beads (PEI-CB and PEI-CSB) formed by 5 g PEI/100 ml of DMA were used for all adsorption experiments. Aliquots were carefully withdrawn from the solutions at predetermined time intervals up to 24 h, and the RB5 concentration (C) in the experimental solution (mg/l) was determined from the calibration curve prepared by measuring the absorbance of different predetermined concentrations of RB5 solutions at λ_{max} 597 nm using a DR5000 spectrophotometer (HACH, USA). The amount of adsorbed dye on the adsorbents (mg/g) was calculated according to the following mass balance equation:

$$q = \frac{(C_0 - C_{eq}) \times V}{W} \quad (1)$$

where q is the amount of dye adsorbed by the adsorbent (mg/g); C_0 and C_{eq} are the initial and equilibrium liquid phase concentrations of RB5 (mg/l); V is the volume of dye solution (l); and W is the dry weight of the beads (g).

2.5. Adsorption isotherm models

The adsorption capacities of CB, PEI-CB, CSB and PEI-CSB for RB5 were evaluated by fitting the equilibrium isotherm data to the Langmuir and Freundlich isotherm models, and these models were statistically analyzed by the non-linear coefficients of determination (R^2) and a non-linear Chi-square test (χ^2).

The Langmuir model is represented as:

$$q_e = \frac{q_m K_L C_e}{1 + K_L C_e} \quad (2)$$

where C_e is the equilibrium concentration of RB5 (mg/l) in the solution, q_e is the equilibrium RB5 concentration (mg/g) on the adsorbent and q_m (mg/g) and K_L (l/mg) are Langmuir constants related to the maximum adsorption capacity of the adsorbents and the affinity between the adsorbate and adsorbents, respectively. The value q_m indicates the complete monolayer coverage of the adsorbent.

The essential features of the Langmuir isotherm can be expressed in terms of a dimensionless constant term (R_L):

$$R_L = \frac{1}{1 + K_L C_0} \quad (3)$$

R_L values within the range $0 < R_L < 1$ indicate favorable adsorption.

The expression of the Freundlich model is:

$$q_e = K_F C_e^{(1/n)} \quad (4)$$

K_F [(mg/g)/(mg/l)$^{1/n}$] is the Freundlich constant related to the adsorption capacity of CSB, and n is an empirical parameter representing the affinity of adsorbent and adsorbate molecules.

3. Results and discussion

3.1. General properties of PEI-grafted CB (PEI-CB) and PEI-grafted CSB (PEI-CSB)

Fig. 1 represents the schematic diagram of the grafting of PEI onto CS beads using ECH as a cross-linker. As shown in the diagram, CS-PEI cross-linking sites on the beads were generated though ECH cross-linker and ECH was selected as a cross-linker here because ECH binds much more preferentially with O–H groups of CS than its amine groups ($-NH_2$) [19]. Thereby, $-NH_2$ groups of CS are not blocked significantly and also, the adsorption capacity of CS beads for dye (RB5) would not be reduced by the cross-linking step using ECH during grafting of PEI.

The white color of CB as well as CSB turned into yellowish after PEI grafting using ECH as cross-linker. The size of CB was found 3.50 mm and after PEI grafting, the size of PEI-CB was increased to 3.90 mm. The size of CSB (2.70 mm) was found less than that of CB,

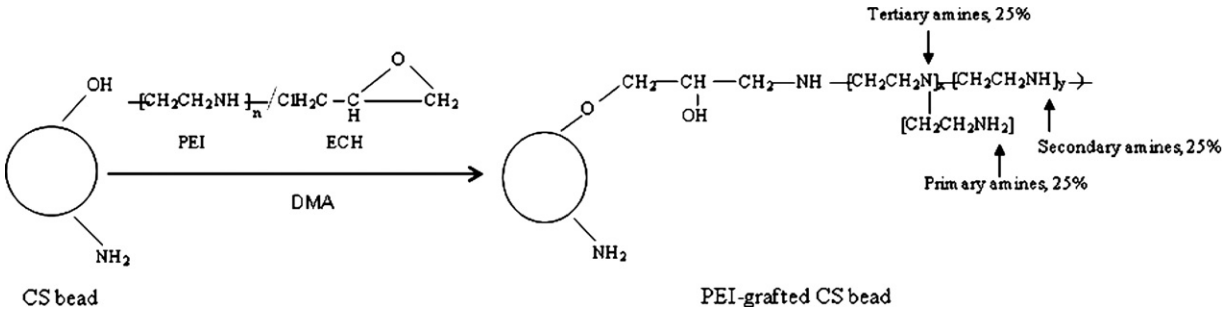

Fig. 1. A schematic diagram of PEI grafting onto CS beads using ECH as a cross-linker.

and after PEI grafting, the size of CSB-PEI (2.80 nm) was also found much less than that of CB-PEI. Thereby, PEI grafting increased the size of the beads. The values of dry weight (g)/wet weight (g) of CB and PEI-CB were 0.033 and 0.070, respectively, indicating more than 2 times of dry weight (g)/wet weight (g) increase of beads after PEI grafting, and the water content PEI-CB (93.0%) was less than that of CB (96.5%), suggesting that PEI grafting made beads more denser than CB. The values of dry weight (g)/wet weight (g) of CSB and PEI-CSB were 0.037 and 0.051, indicating that the dry weight (g)/wet weight (g) increase of CSB after PEI grafting was <1.5 times and the water contents of those beads were 96.3%, and 94.9%, respectively. Thereby, these values indicated that the material content of CB could be increased in much higher amount than that of CSB by PEI grafting.

The porosity (ε) of the beads could be determined by the equation using the amount of water within the pores of the beads [19].

$$\varepsilon = \frac{(W_W - W_D)/\rho_W}{W_D/\rho_{Mat} + (W_W - W_D)/\rho_W} \times 100\% \quad (5)$$

where W_W (g) is the weight of the wet beads before drying; W_D (g) is the weight of the beads after drying; ρ_w is the density of water, 1.0 g/cm^3; and ρ_{Mat} (g/cm^3) is the material density of dry bead. The mean wet weight and dry weight of 3 sets of 10 beads gave the W_W (g) and W_D (g) of a single bead. The value of ρ_{Mat} (g/cm^3) was determined from the ratio of the dry weight of bead/volume of the dry materials of the beads. The values of ρ_{Mat} for CB, and PEI-CB were 0.193 and 0.477 g/cm^3, respectively, indicating that material density of dry beads was higher for PEI-CB than that of CB. The value of ε for PEI-CB (86.27%) was higher than that of CB (85.04%). PEI-CSB (0.344 g/cm^3) showed higher value of ρ_{Mat} than CSB (0.196 g/cm^3) and ε of PEI-CSB (86.48%) calculated from the equation was higher than that of CSB (83.64%). Thereby, the porosity of CB as well as CSB was increased after PEI grafting.

3.2. Determination of PEI and cross-linking ratio of ECH in polyaminated CS beads

Table 1 exhibits the main characteristics of CB and CSB obtained during PEI grafting. The impregnation of 5 g of CB with 5 g PEI/100 ml of DMA solution led to an increase in the dry weight of CB by 19.7 mg (for 100 beads), from 45.5 mg (100 CB) to 65.2 mg (100 PEI-CB$_1$) and the increase in dry weight of the beads after this treatment indicated incorporation of PEI in the beads. After cross-linking with ECH, the dry weight increased by 21.9 mg, from 65.2 mg (100 PEI-CB$_1$) to 87.1 mg (100 PEI-CB$_2$) and this indicated further dry weight increase of beads due to ECH incorporation. Thereby, the wt% of PEI in PEI-CB$_2$ was determined from the ratio of dry weight increase due to PEI incorporation in the PEI-CB$_1$ to dry weight of PEI-CB$_2$ and it was found to be 22.62%. The molar value of NH_2 of the CS/g dry weight of CB was determined 0.0053 because CB was considered of comprising only CS molecules with 85% deacetylation and the molecular weight of glucosamine units is 161 g/mol. Thereby, the molar value of NH_2 of the CS/g dry weight of PEI-CB$_2$ was determined to be 0.0028. The cross-linking ratio (CLR) in PEI-CB$_2$ was determined based on mol ECH:mol NH_2 of CS in PEI-CB$_2$ and the cross-linking ratio was found 0.97. Table 1 also shows that the PEI grafting of CB with 1, 2.5, 10 and 15 g PEI/100 ml of DMA solution, and the results indicated that the amount of PEI in the beads increased with the amount of PEI in DMA solution during the PEI impregnation step up to 15 g PEI/100 ml of DMA. The CLR was found to increase significantly up to 10.0 g PEI/100 ml of DMA solution, and after that, no significant change in the CLR value was found. As shown in Table 1, the dry weight of CS during the formation of PEI-CB$_2$ was always constant (45.5 mg for 100 beads) and the increase in dry weight of beads during the formation of PEI-CB$_1$ from CB, and from PEI-CB$_1$ to PEI-CB$_2$, was due to the incorporation of PEI and ECH, respectively. Depending on the PEI grafting conditions, the dry weight of PEI-CB increased with increase in PEI

Table 1
PEI amount and cross-linking ratio of ECH in PEI-CB or PEI-CSB.

Type	PEI grafting[a]	Sample[b]	B_W (mg)	PEI_W (mg)	ECH_W (mg)	CLR
		CB	45.5	–	–	–
	1	PEI-CB$_1$	52.3	6.8	–	–
		PEI-CB$_2$	66.7	6.8	14.4	0.65
		CB	45.5	–	–	–
	2.5	PEI-CB$_1$	60.9	15.4	–	–
		PEI-CB$_2$	81.6	15.4	20.7	0.91
		CB	45.5	–	–	–
PEI-CB	5	PEI-CB$_1$	65.2	19.7	–	–
		PEI-CB$_2$	87.1	19.7	21.9	0.97
		CB	45.5	–	–	–
	10	PEI-CB$_1$	73.9	28.4	–	–
		PEI-CB$_2$	97.1	28.4	23.2	1.08
		CB	45.5	–	–	–
	15	PEI-CB$_1$	75.8	30.3	–	–
		PEI-CB$_2$	99.5	30.3	23.7	1.08
		CSB	49.7	–	–	
	1	PEI-CSB$_1$	53.8	4.1	–	
		PEI-CSB$_2$	62.2	4.1	8.4	0.79
		CSB	49.7	–	–	
	2.5	PEI-CSB$_1$	58.1	8.4	–	
		PEI-CSB$_2$	69.6	8.4	11.5	1.06
		CSB	49.7	–	–	
PEI-CSB	5	PEI-CSB$_1$	60.2	10.5	–	
		PEI-CSB$_2$	72.0	10.5	11.8	1.06
		CSB	49.7	–	–	
	10	PEI-CSB$_1$	60.4	10.7	–	
		PEI-CSB$_2$	71.9	10.7	11.5	1.00
		CSB	49.7	–	–	
	15	PEI-CSB$_1$	60.3	10.6	–	
		PEI-CSB$_2$	72.1	10.6	11.8	1.06

[a] PEI amount (g)/100 ml of DMA solution for grafting 5 g wet CB or CSB.
[b] 100 CB or CSB; PEI-CB$_1$ or PEI-CSB$_1$, before ECH cross-linking; PEI-CB$_2$ or PEI-CSB$_2$, after ECH cross-linking; B_W, dry weight of beads (mg); PEI_W, PEI weight (mg) in beads; ECH_W, ECH weight (mg) in beads; CLR, cross-linking ratio (mol ECH:mol NH_2 of CS) in beads.

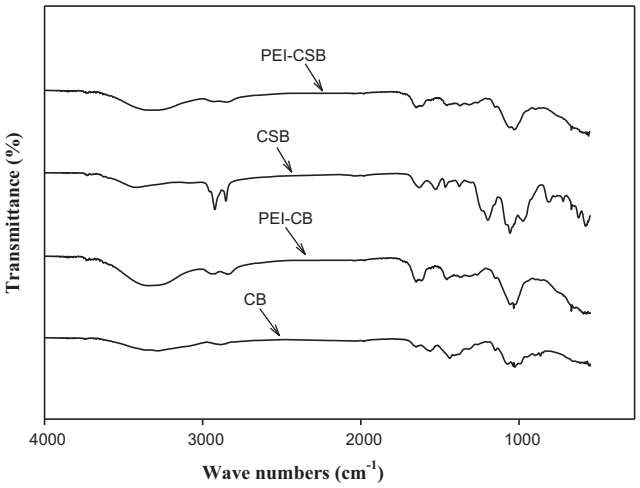

Fig. 2. FTIR spectra of CB and CSB before and after PEI grafting.

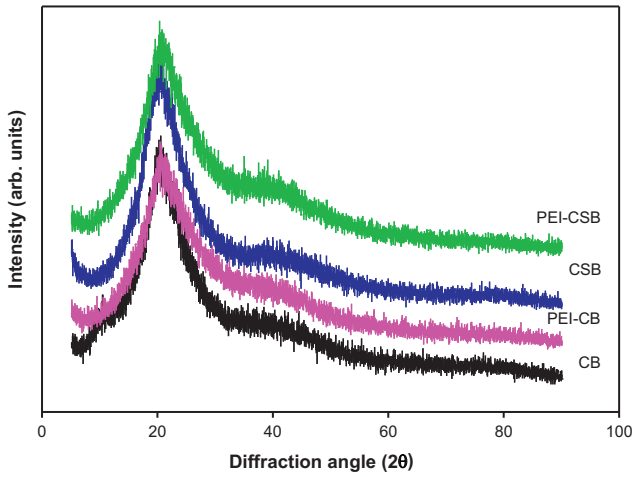

Fig. 3. X-ray diffraction (XRD) patterns of CB and CSB before and after PEI grafting.

concentration in DMA solution. However, the CLR (mol ECH:mol NH_2 of CS) value of PEI-CB_2 after 10 g PEI/100 ml DMA solution did not change because the dry weight increase of PEI-CB_2 with increase in PEI concentration in DMA solution after 10 g PEI/100 ml DMA could not change the CLR value of PEI-CB_2.

The impregnation of 5 g CSB with 5 g PEI/100 ml of DMA solution led to an increase in the dry weight of CSB by 10.5 mg (for 100 beads), from 49.7 mg (100 CSB) to 60.2 mg (100 PEI-CSB_1). After cross-linking with ECH, the dry weight increased by 11.8 mg, from 60.2 mg (100 PEI-CSB_1) to 72.0 mg (100 PEI-CSB_2). Thereby, the wt% of PEI in PEI-CSB_2 was 13.80%. The SDS and CS content of CSB was 0.553 and 0.447 g/g dry weight of bead, respectively, and the molar value of NH_2 in the CS/g dry weight of CSB formed by 5 g/l SDS gelation was 0.0024, as reported in an earlier publication [10]. Thereby, the molar value of NH_2 in the CS/g dry weight of PEI-CSB_2 formed by 5 g/l SDS gelation was 0.0017. Based on this value, the cross-linking ratio (mol ECH:mol NH_2 of CS) in PEI-CSB_2 was 1.06. PEI grafting of CSB with various PEI concentrations indicated that both the amount of PEI in the beads and the cross-linking ratio increased only up to 2.5 g PEI/100 ml of DMA solution, and after that, no significant change in the values was found. No change in the CLR value of PEI-CSB_2 after 2.5 g PEI/100 ml DMA solution could be due to the fact that PEI concentration above 2.5 g PEI/100 ml DMA solution could not further increase the value of mol ECH:mol NH_2 of CS in PEI-CSB_2 even though dry weight of PEI-CSB_2 was increased. Moreover, this earlier saturation of PEI and ECH in CSB compared to CB seems to be reasonable because CSB has denser gel structure than CB.

3.3. Characterization of PEI-grafted CB (PEI-CB) and PEI-grafted CSB (PEI-CSB)

As shown in Fig. 2, the characteristic peaks assignment of CB are: 3283 cm^{-1} (wide peak of O–H stretching overlapped with N–H stretching), 2884 cm^{-1} (C–H stretching), 1560 cm^{-1} (amide II band, N–H bending and C=O stretching of acetyl groups), 1438 cm^{-1} (O–H bending, C–N stretching, asymmetric C–H bending of CH_2 group), and 1038 cm^{-1} (bridge C–O–C stretching and C–O stretching). The characteristic peaks obtained for PEI-CB are: 3337 cm^{-1} (wide peak of O–H stretching overlapped with N–H stretching), 2844 cm^{-1} (C–H stretching), 1653 cm^{-1} (amide II band, N–H bending and C=O stretching of acetyl groups), 1457 cm^{-1} (O–H bending, C–N stretching, asymmetric C–H bending of CH_2 group), and 1033 cm^{-1} (bridge C–O–C stretching and C–O stretching). The peak at 3283 cm^{-1} for CB has shifted to higher wave number (3337 cm^{-1}) with more intensity after PEI grafting, indicating that the density of N–H groups in CB are enhanced after PEI grafting. The peak at 2884 cm^{-1} for C–H stretching in CB is shifted to lower wave number (2844 cm^{-1}) with higher peak intensity in PEI-CB. The other significant changes are noted at 1560–1653 cm^{-1}, 1438–1457 cm^{-1} and 1038–1033 cm^{-1} after PEI grafting. These spectral changes indicate that PEI molecules are grafted into CB through ECH cross-linking and this interaction mainly occurs through interaction with hydroxyl groups of CS molecules during grafting because ECH more prefers O–H than N–H of CS molecules during cross-linking.

Fig. 2 shows that the characteristic peaks assigned for CSB are: 3425 cm^{-1} (wide peak of O–H stretching overlapped with N–H stretching), 2923 and 2853 cm^{-1} (C–H stretching), 1630 and 1527 cm^{-1} (amide II band, N–H bending and C=O stretching of acetyl groups), 1466 cm^{-1} (asymmetric C–H bending of CH_2 group), 1377 cm^{-1} (O–H bending and C–N stretching) and 1057 cm^{-1} (bridge C–O–C stretching and C–O stretching). The appearance of spectral peaks at 2923 and 2853 cm^{-1}, and in the region between 1650 and 1500 cm^{-1} indicates binding of SDS molecules with N–H group of CS molecules during gelation. The characteristic peaks obtained for PEI-CSB are: 3307 cm^{-1} (wide peak of O–H stretching overlapped with N–H stretching), 2845 cm^{-1} (C–H stretching), 1647 cm^{-1} (amide II band, N–H bending and C=O stretching of acetyl groups), 1375 cm^{-1} (O–H bending and C–N stretching) and 1031 cm^{-1} (bridge C–O–C stretching and C–O stretching). The appearance of wider and higher intensity spectral peaks of PEI-CSB at 3307 cm^{-1} than that of CSB at 3425 cm^{-1} indicates that number of N–H groups in CSB is enhanced after PEI grafting (PEI-CSB). The intensity of spectral peak assigned for C–H stretching is decreased after PEI grafting and two spectral peaks at 2923 and 2853 cm^{-1} in CSB reduces to one spectral peak at 2845 cm^{-1} in PEI-CSB. Moreover, the two peaks assigned for C=O stretching of acetyl groups at 1630 and 1527 cm^{-1} in CSB become one peak at 1647 cm^{-1} in PEI-CSB. The other change in spectral peak is noted at 1057–1031 cm^{-1} after PEI grafting in CSB. Thereby, FTIR results clearly suggest that PEI is successfully grafted into CSB using ECH as a cross-linker in this study.

As shown in Fig. 3, the XRD patterns of CB and its PEI grafted derivative (PEI-CB), as well as CSB and its PEI grafted derivative (PEI-CSB) show broad peak at 2θ of 20°. Native CS gives two characteristic crystallinity peaks at 2θ of 10 and 20° (data not shown), however only one broad peak at $2\theta = 20°$ implies decrease in the crystallinity of the CS based hydrogel beads (CB and CSB) and suggests the existence of an amorphous structure in the samples. Also, the similar XRD pattern of PEI-CB and PEI-CSB, as well as CB and CSB in this study indicates that PEI grafting does not affect the crystalline structure of original beads.

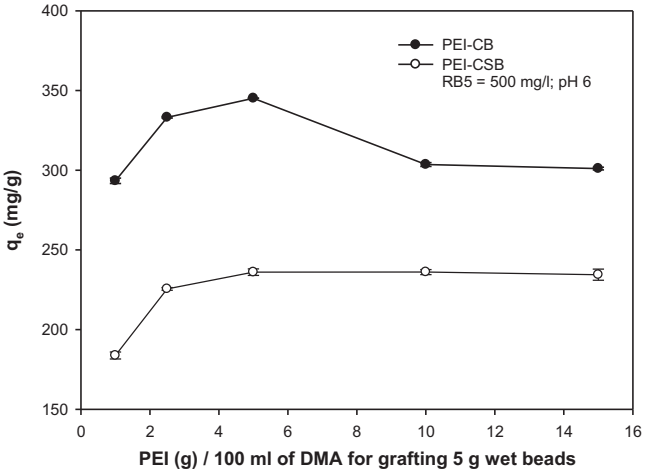

Fig. 4. Effect of PEI grafting on the adsorption capacities of CB and CSB for RB5 adsorption; initial RB5 concentration, 500 mg/l and pH 6.

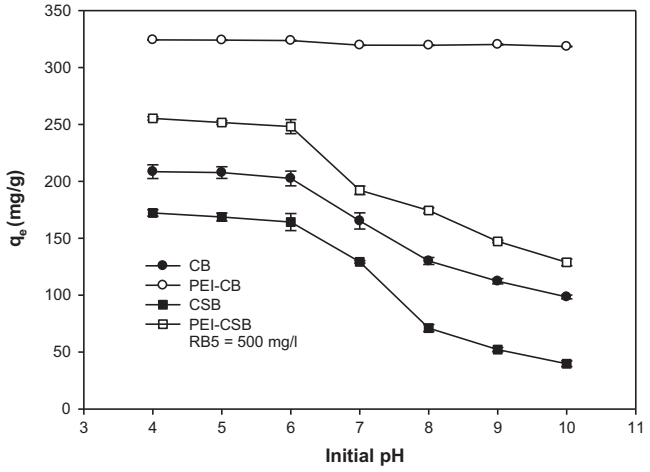

Fig. 5. Effect of initial pH of RB5 solution on its adsorption onto CB and CSB and their polyaminated derivatives PEI-CB and PEI-CSB; RB5 concentration, 500 mg/l.

3.4. Effect of PEI grafting

As shown in Table 1, PEI_w (mg) of 100 PEI-CBs increased from 6.8 to 30.3 mg with increasing 1–15 PEI g/100 ml of DMA for grafting 5 g wet CB, and this was reflected in the adsorption capacity of PEI-CB for the adsorption of 500 mg/l RB5; the results are shown in Fig. 4. The adsorption capacity of PEI-CB increased up to 5 g PEI/100 ml of DMA solution, from 293.34 mg/g to 345.17 mg/g, and after that, it decreased from 345.17 mg/g to 301.04 mg/g with an increase in PEI amount up to 15 g PEI/100 ml of DMA solution during grafting, indicating that increased PEI_w (mg) of PEI-CB gave rise to a higher number of binding (aminated) sites. The increased adsorption capacity of PEI-CB for RB5 up to 5 g PEI/100 ml of DMA solution might be due to increased number of available binding sites for RB5. After that, the steric hindrance between the binding sites increased because of increased numbers of cross-linking sites of PEI-CB through ECH cross-linking with an increase in PEI amount during grafting and that, in turn, reduced the number of available spaces for RB5 molecules.

Table 1 shows that the PEI_w (mg) of 100 PEI-CSB increased from 4.1 to 10.5 mg with increasing 1–5 PEI g/100 ml of DMA for grafting 5 g wet CSB. As shown in Fig. 4, the adsorption capacity (q_e) of PEI-CSB increased from 183.77 to 236.05 mg with the same amount of PEI grafting, and that could be explained by the increase in available binding (aminated) sites by increasing PEI amount during grafting. The PEI_w (mg) of 100 PEI-CSB did not increase significantly with further increase of PEI beyond 5 PEI g/100 ml of DMA during grafting, and a similar adsorption capacity (q_e) of PEI-CSB was found with PEI concentrations of 5, 10 and 15 PEI g/100 ml of DMA; this indicates that the shell membrane structure of CSB limited the amount of PEI during grafting.

As shown in Table 1, the amount of PEI grafted in CSB (PEI-CSB) was less than that in PEI-CB, and in some cases, especially in the grafting conditions of 5, 10 and 15 PEI g/100 ml of DMA, the amount of PEI incorporated in PEI-CSB was <46.7%, 62.3%, and 65.0% of that in PEI-CB, respectively. The shell membrane structure of CSB mainly limited the incorporation of PEI into the beads and so, the numbers of binding sites in PEI-CSB were expected to be much less than that in PEI-CB. Thereby, the more number of available binding sites in PEI-CB than PEI-CSB could be the possible reason for the larger RB5 adsorption on PEI-CB than on PEI-CSB in this study.

3.5. Effect of pH

Fig. 5 shows the effect of the initial pH of the RB5 solution on the adsorption capacities of CB and CSB formed by 5 g/l SDS gelation and their polyaminated derivatives PEI-CB and PEI-CSB, respectively. The initial pH range, from 4 to 10, was selected for this study with an initial RB5 concentration of 500 mg/l. The pH change during adsorption was not adjusted by adding acid or alkali externally and was measured at different time intervals during adsorption. With an initial pH of 5, the pH change during adsorption was measured and was only found within the first 1 h. The pH change of the dye from an initial pH of 5–6 indicated that the protonation of amine groups on the beads occurs during adsorption, but no significant pH change during adsorption was found when the initial pH of RB5 solution was fixed either at pH 7 or 9. PEI-CB exhibited almost similar adsorption capacity at all pH levels (pH 4–10) in this study, and its adsorption capacity decreased slightly from 324.24 to 318.43 mg/g with an increase in the initial pH from 4 to 10. The adsorption capacities of PEI-CSB were almost similar at all acidic pH levels: 255.31 mg/g (pH 4), 251.65 mg/g (pH 5) and 248.06 (pH 6). The pH change to neutral and basic levels significantly decreased the adsorption capacity of PEI-CSB, and its adsorption capacity at pH 7 and 10 were 192.18 and 128.84 mg/g, respectively. In fact, the adsorption capacity of PEI-CB was found to be higher than that of PEI-CSB at all pH levels tested in this study and the effective pH range of PEI-CB for adsorption of RB5 was higher than that of PEI-CSB. The pK_a (10.5) of PEI is higher than that of CS (6.5), and the higher the pK_a value of the ligand (PEI) grafted onto the adsorbent, the wider is the effective pH range for anionic dye adsorption [24]. As shown in Table 1, PEI amount in PEI-CB was much more than that in PEI-CSB and so, the adsorption capacity of PEI-CB showed less sensitivity to pH change of dye solution than that of PEI-CSB because of the higher amount of PEI grafted in PEI-CB than that in PEI-CSB. Moreover, the low adsorption capacity of PEI-CSB at basic pH levels was due to enhanced electrostatic repulsion between ionized SDS molecules and anionic dye (RB5) molecules. Both CB and CSB exhibited maximum adsorption capacity at an initial pH of 4 due to enhanced electrostatic interactions between the positively charged amine groups of CS and RB5 molecules, and the adsorption capacities of the beads decreased with an increase in the initial pH of the dye solution because pH affects the surface charges of CS molecules of CS and CSB.

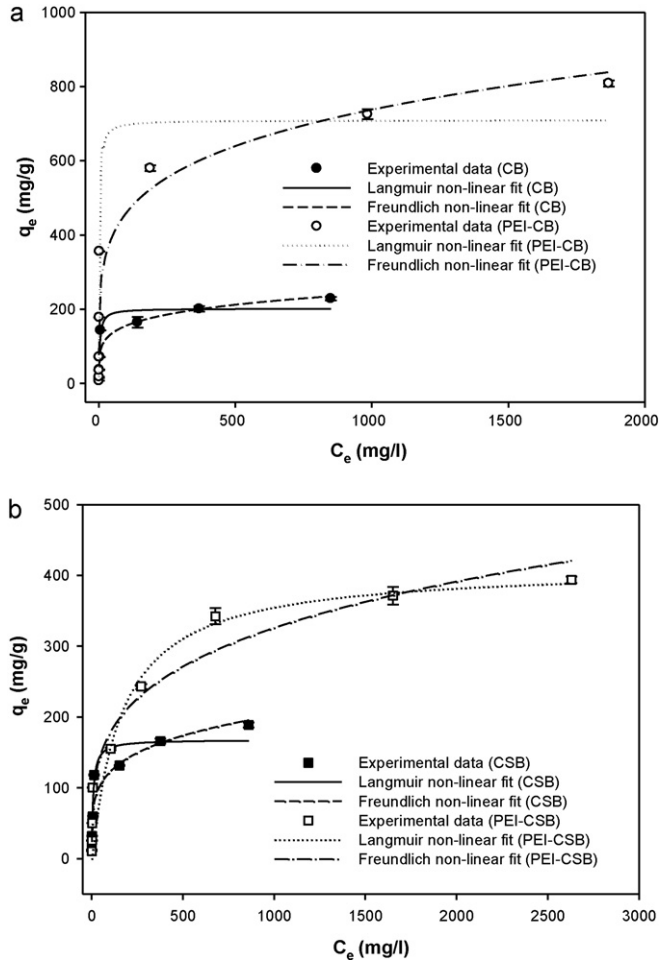

Fig. 6. Plots of q_e vs. C_e for the adsorption of RB5 onto CB, PEI-CB (a), CSB and PEI-CSB (b); pH 6 and 30 °C.

3.6. Equilibrium adsorption isotherm

Fig. 6a and b exhibits the fitting of adsorption isotherm data of CB and its PEI derivative (PEI-CB) and CSB and its PEI derivative (PEI-CSB) to the Langmuir and Freundlich isotherm models, respectively. The constant terms of these isotherm models and the non-linear R^2 and χ^2 values are given in Table 2. The q_{max} values of PEI-CB and PEI-CSB obtained from the Langmuir model were 709.27 and 413.23 mg/g, respectively. The results for R^2 (0.968) and χ^2 (42.44) of the Langmuir model and R^2 (0.934) and χ^2 (350.17) of the Freundlich model for PEI-CB suggested that the Langmuir isotherm model exhibited a better fit to the isotherm data of PEI-CB than did the Freundlich isotherm model. The results for the non-linear R^2 and χ^2 values of the Langmuir (0.945 and 2029.44) and Freundlich (0.973 and 40.62) models for adsorption of RB5 onto PEI-CSB indicated that the adsorption isotherm data of PEI-CSB showed a better fit to the Freundlich model than to the Langmuir model. The K_F and n values of PEI-CSB obtained from the Freundlich model were 52.59 and 3.788. The Langmuir isotherm model appears to be the best-fitting model for CB and CSB because it gives the highest correlation coefficient (R^2) and lowest Chi-square (χ^2) values. The maximum adsorption capacity (q_{max}) values of CB and CSB obtained from the Langmuir isotherm model were 201.90 and 168.07 mg/g, respectively. Thereby, the maximum adsorption capacity of CB and CSB for RB5 could be highly improved by PEI grafting, and their polyaminated derivatives PEI-CB and PEI-CSB exhibited better adsorption capacity than unpolyaminated CB and CSB.

Table 2
Constants for equilibrium isotherm models with error analysis values.

Langmuir isotherm model Adsorbent	K_L (l/mg)	q_{max} (mg/g)	R_L[a]	R^2	χ^2
CB	0.287	201.90	0.004	0.933	26.74
PEI-CB	0.565	709.27	0.002	0.968	42.44
CSB	0.135	168.07	0.007	0.937	16.88
PEI-CSB	0.006	413.23	0.143	0.945	2029.44

Freundlich isotherm model Adsorbent	K_F [(mg/g)/(mg/l)$^{1/n}$]	n	R^2	χ^2
CB	64.45	5.208	0.896	59.82
PEI-CB	178.62	4.878	0.934	350.17
CSB	44.91	4.587	0.909	41.60
PEI-CSB	52.59	3.788	0.973	40.62

[a] C_0 is 1000 mg/l.

Table 3
Comparison of maximum adsorption capacities (q_{max}) of various adsorbents for RB5.

Type of adsorbent	q_{max} (mg/g)	Reference
High lime flyash	7.18	[25]
Cetyltrimethylammonium bromide modified zeolite	12.93	[26]
Powdered activated carbon	58.82	[27]
Bone char	157.00	[28]
Bamboo carbon (2123 m^2/g)	447.00	[28]
Bamboo carbon (1400 m^2/g)	545.00	[28]
CS (<710 μm)	1000.00	[22]
Preprotonated CS (<710 μm)	750.00	[22]
Magnetic CS resin	773.62	[29]
Glutaraldehyde-crosslinked CS microparticles	1680.80	[30]
Templated ECH-crosslinked CS microparticles	2941.00	[31]
Activated sludge biomass	116.00	[32]
0.1 M NaOH treated *Aspergillus foetidus* biomass	106.40	[33]
Brown seaweed, *Laminaria* sp.	101.50	[34]
Corynebacterium glutamicum biomass	185.2	[35]
PEI-CB	709.27	Present work
PEI-CSB	413.23	Present work

As shown in Table 3, the comparison of the maximum adsorption capacities of PEI-CB (709.27 mg/g) and PEI-CSB (413.23 mg/g) for RB5 with that of other adsorbents such as 7.18 mg/g of high lime flyash [25], 12.93 mg/g of cetyltrimethylammonium bromide-modified zeolite [26], 58.82 mg/g of powdered activated carbon [27], 157.00 mg/g of bone char [28], 447.00 mg/g of bamboo carbon (2123 m^2/g) [28], 545.00 mg/g of bamboo carbon (1400 m^2/g) [28], 1000 mg/g CS (<710 μm) and 750 mg/g preprotonated CS (<710 μm) [22], 773.62 mg/g of magnetic CS resin [29], 1680.80 mg/g of glutaraldehyde-crosslinked CS microparticles [30], 2941.00 mg/g of templated ECH-crosslinked CS microparticles [31], 116.00 mg/g of activated sludge biomass [32], 106.40 mg/g of 0.1 M NaOH-treated *Aspergillus foetidus* biomass [33], 101.50 mg/g of Brown seaweed, *Laminaria* sp. [34], and 185.20 mg/g of *Corynebacterium glutamicum* biomass [35] indicated that polyaminated derivatives of CB (PEI-CB) and CSB (PEI-CSB) are very effective in the adsorption of RB5 from aqueous solutions; these materials have promising potential as adsorbents for environmental field applications.

3.7. Volumetric adsorption capacity

Table 4 shows the density and volumetric adsorption capacities of CB and its PEI derivative (PEI-CB) as well as membrane materials of CSB (CSM) and its PEI derivative (PEI-CSM). As shown in Table 4, the density values of CB and PEI-CB were 0.023 and 0.036 g dry weight/ml bead, and their volumetric adsorption capacities

Table 4
Volumetric adsorption capacities of different type adsorbent materials.

Type	Density of materials (g/ml)	Maximum adsorption capacity (q_{max}) (mg RB5/g dry weight)	Volumetric adsorption capacity ($q_{max,v}$) (mg RB5/ml material)
CB	0.023	212.77	4.89
PEI-CB	0.036	709.27	25.53
CSM[a]	0.450	185.19	83.34
PEI-CSM[a]	0.514	413.23	212.40

[a] CSM and PEI-CSM were the membrane materials of CSB and PEI-CSB, respectively.

were 4.89 and 25.53 mg RB5/ml bead, respectively, indicating that PEI-CB exhibited 5.22 times higher volumetric adsorption capacity than raw CB. Membrane materials of CSB (CSM) and its PEI derivative (PEI-CSM) were obtained after squeezing core water from CSB and PEI-CSB, and the volumetric adsorption capacity of membrane materials (mg RB5/ml membrane material) was obtained by multiplying q_{max} (mg/g) by g dry weight/ml of the membrane materials. The density and volumetric adsorption capacity values of CSM and PEI-CSM were 0.450 and 0.514 g/ml membrane material and 83.34 and 212.40 mg RB5/ml membrane material, respectively, indicating that membrane materials of PEI derivatives (PEI-CSM) exhibited 2.55 times higher volumetric adsorption capacity than their raw form (CSM). More interestingly, the volumetric adsorption capacity of PEI-CSM (212.40 mg RB5/ml membrane material) was 8.32 times higher than the volumetric adsorption capacity of PEI-CB (25.53 mg RB5/ml bead). Therefore, significant enhancement of the volumetric adsorption capacity of PEI-CSM could enhance the applicability of polyaminated derivatives of CSB in actual wastewater treatment.

3.8. Kinetic study

The experimental kinetic data of CB and its PEI derivative (PEI-CB), as well as CSB and its PEI derivative (PEI-CSB), for adsorption of RB5 from a 500 mg/l solution are shown in Fig. 7a and b; the kinetic data were analyzed using pseudo-first-order and pseudo-second-order rate models and an intra-particle diffusion model. The coefficient values of Fig. 7a and b are given in Table 5, and the fitting of experimental kinetic data to rate models has been evaluated by the non-linear coefficients of determination (R^2).

The non-linear form of the pseudo-first-order model is:

$$q_t = q_e(1 - e^{-k1t}) \quad (6)$$

where q_t and q_e are the amounts of RB5 adsorbed (mg/g) at time t and equilibrium, respectively, and k_1 (1/min) is the equilibrium rate constant of this equation.

The non-linear form of the pseudo-second-order rate equation is expressed as:

$$q_t = \frac{q_e^2 k_2 t}{1 + q_e k_2 t} \text{ and } h = k_2 q_e^2 \quad (7)$$

where h represents the initial adsorption rate (mg/g min) and k_2 (g/mg min) is the equilibrium rate constant of the pseudo second-order rate model.

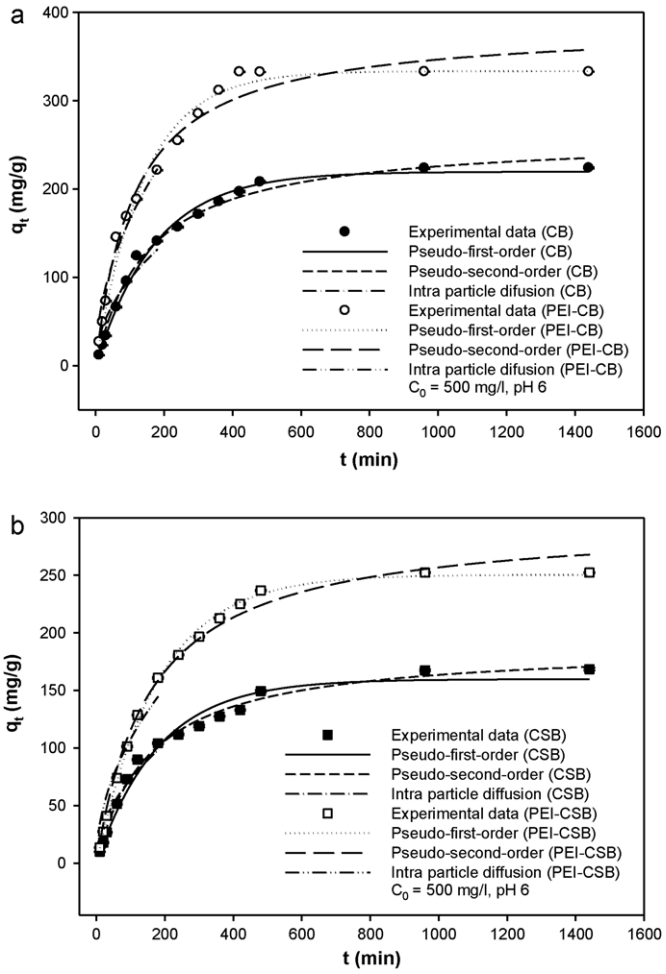

Fig. 7. Plots of q_t vs. t for RB5 adsorption onto CB, PEI-CB (a), CSB and PEI-CSB (b); initial RB5 concentration, 500 mg/l, pH 6.

As shown in Fig. 7a, the non-linear correlation coefficient (R^2) values for the pseudo-first-order and pseudo-second-order rate equations of CB were 0.993 and 0.992, respectively. For PEI-CB, the non-linear R^2 values for the pseudo-first-order and pseudo-second-order equations were 0.986 and 0.981, respectively. The non-linear R^2 values of both rate models for RB5 adsorption onto CB and PEI-CB suggested that the kinetic values of each adsorption system could be better explained by pseudo-first-order rate model than pseudo-second-order rate model. As shown in Fig. 7b, the non-linear R^2 values of CSB for the pseudo-first-order and pseudo-second-order equations were 0.977 and 0.993, indicating that pseudo-second-order rate model could more satisfactorily explain the kinetic data of CSB than pseudo-first-order rate model. The non-linear R^2 values of PEI-CSB for the pseudo-first-order rate and pseudo-second-order rate equations were 0.998 and 0.992, respectively, and based on R^2 values of both rate models for PEI-CSB suggested that kinetic data could be more satisfactorily explained

Table 5
Constants of different rate models for RB5 adsorption with C_0 = 500 mg/l.

Adsorbent	$q_{e\ (exp)}$ (mg/g)	Pseudo-first-order		Pseudo-second-order			Intra particle diffusion
		$q_{e\ (cal)}$ (mg/g)	k_1 (1/min)	$q_{e\ (cal)}$ (mg/g)	k_2 (g/mg min)	h (mg/g min)	k_p (mg/g min$^{0.5}$)
CB	223.95	219.60	5.80×10^{-3}	259.97	2.54×10^{-5}	1.715	9.81
PEI-CB	332.81	333.70	7.20×10^{-3}	385.70	2.31×10^{-5}	3.431	16.60
CSB	168.49	159.78	5.60×10^{-3}	188.92	3.41×10^{-5}	1.217	7.32
PEI-CSB	252.37	250.61	5.60×10^{-3}	297.22	2.14×10^{-5}	1.891	10.78

by pseudo-first-order rate model than pseudo-second-order rate model. The experimental q_e values of CB obtained from the pseudo-first-order and pseudo-second-order rate models were 219.60 and 259.97 mg/g, respectively, and those of PEI-CB were 333.70 and 385.70 mg/g, respectively. As shown in Table 5, the experimental q_e values of CB (223.95 mg/g) and PEI-CB (332.81 mg/g) showed a better fit to the q_e values obtained from the pseudo-first-order rate model than the pseudo-second-order rate model. The experimental q_e value (168.49 mg/g) of CSB was closer to the pseudo-first-order (159.78 mg/g) than the pseudo-second-order (188.92 mg/g) rate model. The experimental q_e value of PEI-CSB (252.37 mg/g) also showed a better fit to the q_e value obtained from the pseudo-first-order rate equation (250.61 mg/g) than the pseudo-second-order rate equation (297.22 mg/g). Thereby, the values of coefficients and non-linear R^2 values of both rate models for all the adsorption systems clearly suggested that the kinetic values of each adsorption system could be more satisfactorily explained by pseudo-first-order rate model than pseudo-second-order rate model.

The intra-particle diffusion equation is given as:

$$q_t = k_p t^{0.5} \quad (8)$$

where k_p is the intra-particle diffusion rate constant (mg/g min$^{0.5}$). The plot of q_t vs. $t^{0.5}$ using the kinetic data up to 180 min exhibited R^2 values of 0.893, 0.940, 0.909 and 0.909 for CB, PEI-CB, CSB and PEI-CSB, respectively, indicating the role of intra-particle diffusion at the initial stage of adsorption. The high values of k_p of CB and CSB and its polyaminated derivatives also suggest that intra-particle diffusion might play a significant role in all of the adsorption systems.

4. Conclusions

In this study, the adsorption capacities of CB and CSB for RB5 were investigated after PEI grafting. The adsorption capacities and grafted amounts of PEI in PEI-CB and PEI-CSB were found to vary with the amount of PEI during grafting. PEI-CB exhibited similar adsorption capacities at all pH levels (4–10) because of the higher pK_a value (10.5) of grafted PEI molecules. The maximum adsorption capacities of the polyaminated derivative of CB (PEI-CB) and CSB (PEI-CSB) were higher than those of CB and CSB, and the maximum adsorption capacities of PEI-CB and PEI-CSB were 709.27 and 413.23 mg/g, respectively.

Acknowledgement

This research was supported by Basic Science Research Program through the National Research Foundation of Korea (NRF) funded by the Ministry of Education, Science and Technology (grant number 2009-0079636).

References

[1] R.S. Blackburn, Natural polysaccharides and their interactions with dye molecules: applications in effluent treatment, Environ. Sci. Technol. 38 (2004) 4905–4909.
[2] N. Daneshvar, A. Oladegaragoze, N. Djafarzadeh, Decolorization of basic dye solutions by electrocoagulation: an investigation of the effect of operational parameters, J. Hazard. Mater. 129 (2006) 116–122.
[3] G. Crini, Non-conventional low-cost adsorbents for dye removal: a review, Bioresour. Technol. 97 (2006) 1061–1085.
[4] K.C. Chen, J.Y. Wu, C.C. Huang, Y.M. Liang, S.C.J. Hwang, Decolorization of azo dye using PVA-immobilized microorganisms, J. Biotechnol. 101 (2003) 241–252.
[5] Q. Sun, L. Yang, The adsorption of basic dyes from aqueous solution on modified peat-resin particle, Water Res. 37 (2003) 1535–1544.
[6] V.K. Gupta, Suhas, Application of low-cost adsorbents for dye removal—a review, J. Environ. Manage. 90 (2009) 2313–2342.
[7] Z. Aksu, Application of biosorption for the removal of organic pollutants: a review, Process Biochem. 40 (2005) 997–1026.
[8] G. Crini, P.M. Badot, Application of chitosan, a natural aminopolysaccharide, for dye removal from aqueous solutions by adsorption processes using batch studies: a review of recent literature, Prog. Polym. Sci. 33 (2008) 399–447.
[9] N.V. Majeti, R. Kumar, A review of chitin and chitosan applications, React. Funct. Polym. 46 (2000) 1–27.
[10] S. Chatterjee, T. Chatterjee, S.H. Woo, A new type of chitosan hydrogel sorbent generated by anionic surfactant gelation, Bioresour. Technol. 101 (2010) 3853–3858.
[11] Y. Lapitsky, E.W. Kaler, Formation of surfactant and polyelectrolyte gel particles in aqueous solutions, Colloid Surf. A 250 (2004) 179–187.
[12] C. Onesippe, S. Lagerge, Study of the complex formation between sodium dodecyl sulfate and chitosan, Colloid Surf. A 317 (2008) 100–108.
[13] M. Thongngam, D.J. McClements, Characterization of interactions between chitosan and an anionic surfactant, J. Agric. Food Chem. 52 (2004) 987–991.
[14] P. Chassary, T. Vincent, E. Guibal, Metal anion sorption on chiotsan and derivative materials: a strategy for polymer modification and optimum use, React. Funct. Polym. 60 (2004) 137–149.
[15] Y. Kawamura, H. Yoshida, S. Asai, H. Tanibe, Breakthrough curve for adsorption of mercury(II) on polyaminated highly porous chitosan beads, Water Sci. Technol. 35 (1997) 97–105.
[16] T.Y. Kim, S.Y. Cho, Adsorption equilibria of reactive dye onto highly polyaminated porous chitosan beads, Korean J. Chem. Eng. 22 (2005) 691–696.
[17] K.C. Gavilan, A.V. Pestov, H.M. Garcia, Y. Yatluk, J. Roussy, E. Guibal, Mercury sorption on a thiocarbamoyl derivative of chiotsan, J. Hazard. Mater. 165 (2009) 415–426.
[18] N. Li, R.B. Bai, C.K. Liu, Enhanced and selective adsorption of mercury ion on chitosan beads grafted with polyacrylamide via surface-initiated atom transfer radical polymerization, Langmuir 21 (2005) 11780–11787.
[19] S. Chatterjee, D.S. Lee, M.W. Lee, S.H. Woo, Nitrate removal from aqueous solutions by cross-linked chitosan beads conditioned with sodium bisulfate, J. Hazard. Mater. 166 (2009) 508–513.
[20] W. Tanthapanichakoon, P. Ariyadejwanich, P. Japthong, K. Nakagawa, S.R. Mukai, H. Tamon, Water Res. 39 (2005) 1347–1353.
[21] T. Robinson, B. Chandran, P. Nigam, Removal of dyes from an artificial textile dye effluent by two agricultural waste residues, corncob and barley husk, Environ. Int. 28 (2002) 29–33.
[22] G. Gibbs, J.M. Tobin, E. Guibal, Influence of chitosan preprotonation on Reactive Black 5 sorption isotherms and kinetics, Ind. Eng. Chem. Res. 43 (2004) 1–11.
[23] S. Torres-Giner, M.J. Ocio, J.M. Lagaron, Development of active antimicrobial fiber based chitosan polysaccharide nanostructures using electrospinning, Eng. Life Sci. 8 (2008) 303–314.
[24] S. Morimoto, M. Sakata, T. Iwata, A. Esaki, C. Hirayama, Preparations and applications of polyethyleneimine-immobilized cellulose fibers for endotoxin removal, Polym. J. 27 (1995) 831–839.
[25] Z. Eren, F.N. Acar, Equilibrium and kinetic mechanism for Reactive Black 5 sorption onto high lime Soma fly ash, J. Hazard. Mater. 143 (2007) 226–232.
[26] D. Karadag, M. Turan, E. Akgul, S. Tok, A. Faki, Adsorption equilibrium and kinetics of Reactive Black 5 and Reactive Red 239 in aqueous solution onto surfactant-modified zeolite, J. Chem. Eng. Data 52 (2007) 1615–1620.
[27] Z. Eren, F.N. Acar, Adsorption of Reactive Black 5 from an aqueous solution: equilibrium and kinetic studies, Desalination 194 (2006) 1–10.
[28] A.W.M. Ip, J.P. Barford, G. McKay, Reactive Black dye adsorption/desorption onto different adsorbents: effect of salt, surface chemistry, pore size and surface area, J. Colloid Interface Sci. 337 (2009) 32–38.
[29] K.Z. Elwakeel, Removal of Reactive Black 5 from aqueous solutions using magnetic chitosan resins, J. Hazard. Mater. 167 (2009) 383–392.
[30] A.-H. Chen, S.-M. Chen, Biosorption of azo dyes from aqueous solution by glutaraldyde-crosslinked chitosans, J. Hazard. Mater. 172 (2009) 1111–1121.
[31] A.-H. Chen, Y.-Y. Huang, Adsorption of Remazol Black 5 from aqueous solution by the templated crosslinked-chitosans, J. Hazard. Mater. 177 (2010) 668–675.
[32] O. Gulnaz, A. Kaya, S. Dincer, The reuse of dried activated sludge for adsorption of reactive dye, J. Hazard. Mater. B134 (2006) 190–196.
[33] R. Patel, S. Suresh, Kinetic and equilibrium studies on the biosorption of Reactive Black 5 dye by *Aspergillus foetidus*, Bioresour. Technol. 99 (2008) 51–58.
[34] K. Vijayaraghavan, Y.S. Yun, Biosorption of C.I. Reactive Black 5 from aqueous solution using acid-treated biomass of brown seaweed *Laminaria* sp., Dyes Pigments 76 (2008) 726–732.
[35] S.W. Won, H.-J. Kim, S.-H. Choi, B.-W. Chung, K.-J. Kim, Y.-S. Yun, Performance, kinetics and equilibrium in biosorption of anionic dye Reactive Black 5 by the waste biomass of *Corynebacterium glutamicum* as a low-cost biosorbent, Chem. Eng. J. 121 (2006) 37–43.